Comparison of observed and simulated tropical climate trends using a forward model of coral $d^{18}O$

D. M. Thompson,[1] T. R. Ault,[1] M. N. Evans,[2] J. E. Cole,[1,3] and J. Emile-Geay[4]

Received 20 May 2011; accepted 30 May 2011; published 19 July 2011.

[1] The response of the tropical Pacific Ocean to future climate change remains highly uncertain, in part because of the disagreement among observations and coupled general circulation models (CGCMs) regarding 20th-century trends. Here we use forward models of climate proxies to compare CGCM simulations and proxy observations to address 20th-century trends and assess remaining uncertainties in both proxies and models. We model coral oxygen isotopic composition ($\delta^{18}O$) in a 23-site Indo-Pacific network as a linear function of sea-surface temperature (SST) and sea-surface salinity (SSS) obtained from historical marine observations (instrumental data) and a multimodel ensemble of 20th-century CGCM output. When driven with instrumental data from 1958 to 1990, the forward modeled corals (pseudocorals) capture the spatial pattern and temporal evolution of the El Niño-Southern Oscillation (ENSO). Comparison of the linear trend observed in corals and instrumental pseudocorals suggests that the trend in corals between 1958 and 1990 results from both warming (60%) and freshening (40%). From 1890 to 1990, the warming/freshening trend in CGCM pseudocorals is weaker than that observed in corals. Corals display a moderate trend towards a reduced zonal SST gradient and decreased ENSO-related variance between 1895 and 1985, whereas CGCM pseudocorals display a range of trend patterns and an increase in ENSO-related variance over the same period. Differences between corals and CGCM pseudocorals may arise from uncertainties in the linear bivariate coral model, uncertainties in the way corals record climate, undersensitivity of CGCMs to radiative forcing during the 20th century, and/or biases in the simulated CGCM SSS fields. **Citation:** Thompson, D. M., T. R. Ault, M. N. Evans, J. E. Cole, and J. Emile-Geay (2011), Comparison of observed and simulated tropical climate trends using a forward model of coral $\delta^{18}O$, *Geophys. Res. Lett.*, *38*, L14706, doi:10.1029/2011GL048224.

1. Introduction

[2] Despite the importance of ENSO to global climate variability, we still lack a clear understanding of how anthropogenic climate change will affect the background state of the tropical Pacific and the amplitude and frequency of ENSO events [e.g., *Vecchi et al.*, 2008]. Instrumental records disagree regarding 20th-century SST trends in the tropical Pacific [e.g., *Vecchi et al.*, 2008], and CGCM projections of future ENSO behavior differ widely [e.g., *Meehl et al.*, 2007]. Comparison of tropical proxy climate records with CGCM output over the 20th century provides a way to assess CGCM simulations and constrain predictions for future changes in the background state of the tropical Pacific and the frequency of ENSO events.

[3] Proxy climate records provide an archive of climate variability, but their spatial and temporal coverage is limited, they often reflect a response to a multivariate climate signal, and they may exhibit variance that is unrelated to climate. These proxy limitations add uncertainty to inverse-based methods for reconstructing past climate variability. Forward modeling of proxy records offers a complementary approach that may curtail the above uncertainties for several reasons. First, it only requires the prediction of the proxy variable. Second, it can be built upon the established dependence of the proxy variable on environmental controls. Finally, it provides a means to directly compare CGCM data and proxy records. For example, previous studies have developed forward models for tree-ring width and isotope composition [e.g., *Roden et al.*, 2000; *Vaganov et al.*, 2006; *Tolwinski-Ward et al.*, 2011] and have used these models to study changes in proxy-climate relationships over time [e.g., *Anchukaitis et al.*, 2006].

[4] The dependence of coral isotopic composition ($\delta^{18}O_{coral}$) on environmental conditions is well established and the signal-to-noise ratio in this proxy is high [e.g., *Fairbanks et al.*, 1997]. Forward modeling of $\delta^{18}O_{coral}$ thus has considerable potential to analyze variations and trends in the tropical Pacific surface ocean climate. For instance, *Brown et al.* [2006] coupled a linear bivariate model for $\delta^{18}O_{coral}$, based on SST and seawater $\delta^{18}O$ ($\delta^{18}O_{sw}$), with an isotope-enabled CGCM to compare model output with three Indo-Pacific coral records between 1950 and 2000. A subsequent study [*Brown et al.*, 2008] used SST and precipitation from a CGCM to compare 'pseudocoral' variability with ENSO variance reconstructed from mid-Holocene corals.

[5] We build on the work of *Brown et al.* [2006, 2008] by comparing observed $\delta^{18}O_{coral}$ with that predicted by a linear bivariate model driven by 20th-century instrumental data and CGCM output. Using a network of 23 coral records spanning the Indo-Pacific, we first compare leading patterns of climate variability in observed $\delta^{18}O_{coral}$ and $\delta^{18}O_{coral}$ modeled from instrumental data. We refer to these forward-modeled $\delta^{18}O_{coral}$ records as pseudocorals, as done by *Brown et al.* [2008]. We then drive the model with each component

[1]Department of Geosciences, University of Arizona, Tucson, Arizona, USA.
[2]Department of Geology and Earth System Science Interdisciplinary Center, University of Maryland, College Park, Maryland, USA.
[3]Department of Atmospheric Sciences, University of Arizona, Tucson, Arizona, USA.
[4]Department of Earth Sciences, University of Southern California, Los Angeles, California, USA.

0094-8276/11/2011GL048224

separately to diagnose the relative importance of salinity and temperature variations in $\delta^{18}O_{coral}$. We use the model's ability to simulate the observed spatial and temporal patterns of $\delta^{18}O_{coral}$ to determine whether a more sophisticated treatment of $\delta^{18}O_{coral}$ is necessary. Finally, we compare 20th-century trends in corals and CGCM pseudocorals and assess the uncertainties in this intercomparison.

2. Forward Model of Coral $\delta^{18}O$

[6] Prior experiments and observations have shown that variability in $\delta^{18}O_{coral}$ depends linearly on calcification temperature and local $\delta^{18}O_{sw}$ at the time of growth [e.g., *Epstein et al.*, 1953], the latter a result of net freshwater flux between the surface ocean and the atmosphere. Furthermore, time series of $\delta^{18}O$ variability derived from fast-growing reef corals are offset from isotopic equilibrium with surface conditions [*Weber and Woodhead*, 1972]. We therefore modeled $\delta^{18}O_{coral}$ variability as anomaly time series relative to the average over the full analysis period (1958–1990 or 1890–1990). Because $\delta^{18}O_{sw}$ measurements are scarce [*LeGrande and Schmidt*, 2006] and the net freshwater flux affects SSS and $\delta^{18}O_{sw}$ proportionately via evaporation and condensation processes [*Cole and Fairbanks*, 1990; *Fairbanks et al.*, 1997], we estimated $\delta^{18}O_{sw}$ from SSS. This yielded the following model for $\delta^{18}O_{coral}$ anomalies:

$$\delta^{18}O_{pseudocoral} = a_1 SST + a_2 SSS, \quad (1)$$

where a_2 was specified through basin-scale $\delta^{18}O_{sw}$ vs. SSS regression estimates (‰/PSU, Table S1 of the auxiliary material [*LeGrande and Schmidt*, 2006]).[1] We specified a_1 based on the experimental and theoretical dependence of oxygen isotopic equilibrium on the temperature of carbonate formation [e.g., *Epstein et al.*, 1953], which has been observed in well-studied coral genera [e.g., *Evans et al.*, 2000; *Juillet-Leclerc and Schmidt*, 2001; *Lough*, 2004]. Although the slope of this relationship may range from −0.10 to −0.34 ‰/°C at individual sites [*Evans et al.*, 2000], studies that synthesized multiple locations report slopes of −0.2 (10 sites [*Evans et al.*, 2000]) and −0.22 ‰/°C (19 sites [*Lough*, 2004]), close to the inorganic slope of −0.22‰/°C. We selected a slope of a_1 = −0.22 (+/−0.02) ‰/°C for the SST- $\delta^{18}O_{coral}$ relationship.

3. Input Datasets

[7] We tested the forward model using SST and SSS from instrumental data products (SST: ERSSTv2, [*Smith and Reynolds*, 2004], ERSSTv3 [*Smith et al.*, 2008], Kaplan ext.v2 [*Kaplan et al.*, 1998], HadISST [*Rayner et al.*, 2003]; SSS: SODA [*Carton and Giese*, 2008], Carton GOA Beta 7 [*Carton et al.*, 2000]). We then ran the forward model with SST and SSS from 20th−century simulations of several AR4 CGCMs, chosen to reflect the range of 20th-century variability, trends, and ENSO skill exhibited by the full suite of AR4 models [e.g., *Meehl et al.*, 2007; *Guilyardi et al.*, 2009]. We used equation (1) and observed or simulated SST and SSS from the nearest gridbox to model monthly $\delta^{18}O$ for each coral site. The latitude/longitude grid resolution ranged from 0.5 × 0.5 (e.g., SODA) to 5 × 5 (e.g., Kaplan ext.v2); when necessary, we regridded data to the same resolution using box averaging. Each monthly pseudocoral series was annually averaged for further analysis. To assess the relative contribution of SST and SSS in $\delta^{18}O_{coral}$, pseudocorals were also modeled using SST and SSS separately (see Table S2 for all combinations tested).

4. Comparison of Observed and Pseudocoral Networks

[8] The observational target was a dataset of 23 annual $\delta^{18}O_{coral}$ anomaly records, spanning ≥90% of the 1850–1990 interval [*Ault et al.*, 2009] (Table S1). Unlike *Ault et al.* [2009], we did not detrend the $\delta^{18}O$ series because the long-term trends were of prime interest. We used singular value decomposition (SVD) of the $\delta^{18}O$ covariance matrix to determine the spatiotemporal patterns of variability within the observed and pseudocoral $\delta^{18}O$ networks over the common time interval, 1958–1990 for the instrumental period and 1890–1990 for the CGCMs. The "rule N" test [*Overland and Preisendorfer*, 1982] was used to identify significant eigenvectors above the "white noise floor" at the 95% confidence level, where the white noise floor represents the expected eigenvalues if there were no spatial structure.

[9] Two significant eigenvectors emerged from the observed coral network, describing ~30 and ~17% of the variance, respectively, over the 1958–1990 period. We interpreted the pattern of these eigenvectors as the signature of ENSO and a secular trend in the observational network, respectively (Figure S1). The secular trend emerged as the first eigenvector over the 1890–1990 period, explaining 28% of the variance, while ENSO was the second eigenvector and explained 17% of the variance. The ENSO and trend patterns were also significant and described the leading fractions of variance in all pseudocoral networks (Table S2). Varimax rotation of the significant principal components (PCs) had no marked effect on ENSO or the trend.

[10] We examined whether instrumental and CGCM pseudocorals captured the leading modes of variability in the observed coral network. To do this, we compared the spatial and temporal patterns of ENSO and the trend between networks over contemporaneous time intervals (see Text S1).

[11] We then compared observed coral and CGCM pseudocoral trends in ENSO-related variance and tropical Pacific "mean state" over the 20th century [after *Meehl et al.*, 2007] (Figure 2 and see Text S1). To calculate the mean state trend (Figure 2, x-axis), we correlated the spatial expression of ENSO with the spatial pattern of the 20th-century trend. We referred to the trend as "El Niño-like" if the spatial pattern of the trend correlated positively with the pattern of warm-phase ENSO [after *Meehl et al.*, 2007]. We then calculated the change in ENSO variability (y-axis) as the ratio of ENSO-related interannual variability between the last half and first half of the analysis period, such that a ratio greater than one indicates an increase in ENSO-related variability. We performed sensitivity analyses for the mean state and ENSO-related variance calculations using randomly selected subsets of sites (for mean state

[1] Auxiliary materials are available in the HTML. doi:10.1029/2011GL048224.

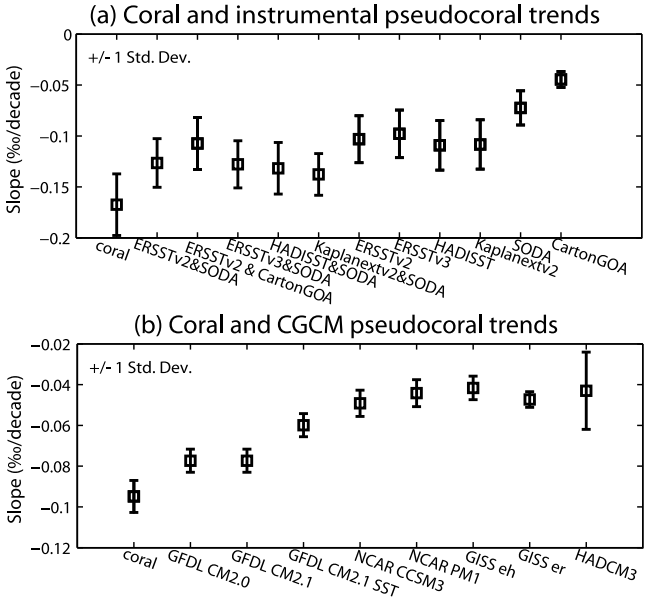

Figure 1. (a) Magnitude of the trend slope (‰/decade, computed from a simple linear regression through the trend PC) in corals (far left) and in instrumental pseudocorals over the 1958–1990 period. Error bars denote ±1 standard deviation. (b) As in Figure 1a but for the trend in corals and CGCM pseudocorals over the 1890–1990 period.

error) and years (for variance error) from the original data set.

5. Results

5.1. Pseudocorals Derived From Instrumental Observations

[12] With one exception (Carton GOA SSS pseudocorals), the ENSO PC from instrumental pseudocorals was significantly related to the ENSO PC from the observed coral network over the 1958–1990 period (Table S2 and Figure S1b). Comparisons of the ENSO PC correlation fields illustrate that instrumental pseudocorals also captured the spatial pattern of ENSO variability over this period (Table S3). We found that for pseudocorals generated with both SST and SSS, the ENSO correlation field differed significantly from the observed coral field in only three (out of ten) cases: HadISST & SODA vs. SST and SSS, and Kaplan ext.v2-SST & SODA vs. SSS (Table S3).

[13] Instrumental pseudocorals also captured the observed trend between 1958 and 1990 (Table S2). The relationship between the observed and pseudocoral trend PCs was strongest for the pseudocoral networks that were modeled with both SST and SSS. Significant relationships between the observed and pseudocoral trend PCs existed despite differing superimposed interannual variability (i.e., the time evolution of the trends), indicating strong consistency of the underlying linear trends. After isolating the linear trend with a linear regression, the residuals were normally distributed around a mean of zero for all instrumental pseudocoral networks. The observed coral trend residuals also displayed a zero mean ($Z = 0.477$, df = 32, $P = 0.684$), despite being positively skewed by the superimposed interannual anomalies. These results indicate that the linear trends, estimated from regression through the trend PCs, were a good fit to the underlying secular trend.

[14] We focused our analysis on the linear trend component as an approximation of the secular trend. This trend toward more negative $\delta^{18}O$ values was significant in all coral networks. Additionally, the RMSE between regression fields of observed and pseudocoral linear trends regressed on SST and SSS were indistinguishable from zero. In both observed corals and pseudocorals, the regression fields suggested that this linear trend reflects increasing SST throughout most of the tropical Indo-Pacific. SSS played an important role in the trend regionally, particularly in the western and southwestern Pacific. Thus, the addition of SSS improved the ability of the model to capture the full magnitude of the observed coral trend between 1958 and 1990 (−0.167 ‰/decade, Figure 1a). This improvement cannot be explained simply by the addition of another component to the model, as the mean trend of 100 pseudocoral networks modeled with SST and noise with the same variance and lag 1 autocorrelation as SSS was similar to that observed in the SST only pseudocoral networks (−0.105 ± 0.018 ‰/decade). Although the magnitude of the coral trend was still about 20% larger than observed in any SST and SSS pseudocoral networks (max of −0.138‰/decade, Figures 1a and S1f), the difference between the observed and pseudocoral trend slopes was not significant. The mean difference between the observed and pseudocoral trend at the 23 coral sites was also not significantly different from zero, suggesting that the linear bivariate model also captured the trends observed at the 23 coral sites. Based on the relative amplitude of the trend in SSS-only and SST-only pseudocorals and that observed over the 1958–1990 period, approximately 40% of the coral trend (−0.045 to −0.072‰/decade) was explained by salinity and approximately 60% of the trend (−0.098 to −0.11 ‰/decade) was explained by temperature.

5.2. Pseudocorals Derived From CGCM Output

[15] Several studies have established that AR4 CGCMs generally simulate the spatial pattern of ENSO, albeit excessively locked to a two-year periodicity [e.g., *Guilyardi et al.*, 2009]. We focused here on trends in the tropical Pacific mean state and in ENSO-related variability because these are harder to constrain using instrumental records alone. As observed in corals, all CGCM pseudocoral networks contained a significant linear trend toward more negative $\delta^{18}O$ values between 1890 and 1990. The linear trend residuals were normally distributed with a mean of zero, indicating again that the linear trend was a good approximation of the underlying secular trend. However, the slope of the linear trend (‰/decade) in all CGCM pseudocoral networks was lower than observed in corals between 1890 and 1990 (Figure 1b). Site by site comparison suggests that this discrepancy may result from weaker trends in the central western Pacific in the CGCM pseudocorals than observed, particularly at Maiana and Jarvis Islands.

[16] We also found that corals and CGCM pseudocorals disagreed regarding 20th-century trends in tropical Pacific mean state and ENSO-related variance (Figure 2). Corals displayed a reduction in ENSO-related variance and a moderate El Niño-like mean state trend. In contrast, CGCM pseudocorals displayed a range of mean state trends and suggested an increase in variance over this same period.

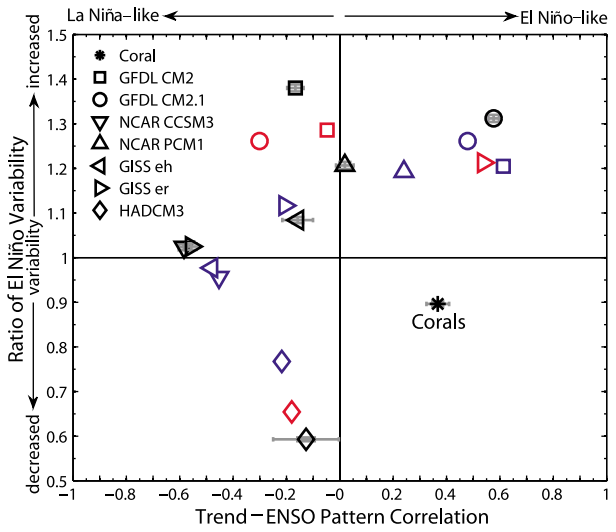

Figure 2. Change in mean state (x-axis) and ENSO-related variability (y-axis) [after *Meehl et al.*, 2007] within the Pacific (120°E to 80°W) between 1895 and 1985 in corals (black asterisk) and CGCM (SST & SSS) pseudocorals (black symbols). The symbols mark the mean and error bars denote the 95% confidence interval of 1000 independently sub-sampled variance ratios and 50 independently sub-sampled pattern correlations. Colored symbols represent analysis of CGCM SST (blue) and SSS (red) at the 23 coral sites. The full CGCM SST field was also analyzed, and the results were similar to that observed at the 23 coral sites. (Note: for CGCMs with no SSS symbol, SSS did not display a significant trend component.)

Although HadCM3 pseudocorals displayed a trend pattern that was most similar to that observed, HadCM3 pseudocorals also showed a much larger reduction in ENSO-related variance than observed, and the trend in HadCM3 pseudocorals over this period was weak (−0.043‰/decade, Figure 1) and sensitive to the selection of sites in the underlying network. When the network included mainly ENSO-sensitive sites, HadCM3 displayed a stronger La Niña-like trend pattern (as in projections of future change [*Meehl et al.*, 2007]).

6. Discussion

[17] Our model captured the spatial and temporal pattern of ENSO and the linear trend observed in corals from 1958 to 1990 and demonstrated that the $\delta^{18}O_{coral}$ trend results from both warming and freshening. These results are consistent with observational studies showing freshening in the tropical Pacific [e.g., *Cravatte et al.*, 2009; *Nurhati et al.*, 2009]. None of the CGCM pseudocoral networks captured the magnitude of the trend, the change in mean state, or the change in ENSO-related variance observed in the coral network over the 1890–1990 period. The negative $\delta^{18}O$ trend was weaker in CGCM pseudocorals than observed, and whereas corals displayed a moderately El Niño-like trend in the Pacific, there was little agreement among CGCMs regarding the spatial pattern of the trend. Finally, the corals displayed a reduction in ENSO-related variance between the first and last half of the analysis period, whereas CGCM pseudocorals generally displayed an increase.

[18] The discrepancies between observed and CGCM pseudocoral trends may stem from uncertainty in the observational coral records, the CGCM output (SST and SSS), and/or the way we translate CGCM output into coral records. Results from sensitivity analyses of the trend pattern suggest that network biases stemming from the site locations and/or time period analyzed are unlikely to have caused this discrepancy, as none of the randomly selected subsets from the CGCM pseudocoral networks overlap with any of the subsets from the observed coral network. Also, the effect of subsampling on the resulting patterns was generally small (see error bars in Figure 2). Finally, it is unlikely that the bivariate linear approximation of the proxy system was the primary cause of the discrepancy, as instrumental pseudocorals were able to capture the interannual variability and trend observed in corals between 1958 and 1990.

[19] Although not significant, the magnitude of the trend was lower in the instrumental pseudocorals than in real corals. This discrepancy appears strongest at sites where instrumental observations are limited (e.g., at the Maiana site), suggesting that these gridded instrumental data products may underestimate SSS and/or SST trends. On the other hand, the discrepancy between observed and pseudocoral trends could be caused by biologically-mediated kinetic isotope effects that may occur in corals under unusually stressful conditions. Although earlier work demonstrated isotopic excursions with extremely slow growth rates [*McConnaughey*, 1989], we have found no relationship between extension rate and $\delta^{18}O$ over the range of growth observed in the corals studied here.

[20] To determine whether the observed-modeled trend discrepancy could be attributed to SST or SSS, the trend-ENSO pattern and ENSO variance analysis was repeated with GCCM temperature and salinity separately at each of the 23 coral sites (Figure 2, colored symbols). The results suggest that SSS played an important role in the simulated trend pattern. The discrepancy between coral and CGCM pseudocoral trends may therefore be driven by differences in the salinity recorded by corals and that simulated by CGCMs. A salinity bias in the coral records, due perhaps to local effects or the way SSS is recorded in corals, is not likely the source of the discrepancy because: (1) the agreement of coral records on a regional scale suggests that local SSS biases on $\delta^{18}O_{coral}$ are minor, (2) the addition of SSS improves the agreement between instrumental pseudocorals and observations, and (3) instrumental pseudocorals and observed corals agree closely.

[21] On the other hand, CGCM SSS often displayed different mean state and ENSO-related variance trends than observed for temperature (Figure 2). Further analyses revealed that the discrepancy between observed corals and CGCM pseudocorals may be caused by biases in the CGCM representation of the hydrological cycle. First, while instrumental SST and SSS displayed a negative relationship throughout most of the tropical Indo-Pacific (Figure 3a), as expected from temperature-driven tropical convection, all but one CGCM analyzed here displayed positive SST-SSS correlations in the eastern and central equatorial Pacific (Figure S2). The average CGCM correlation pattern, weighted by the model's ability to capture tropical climate variability [*Gleckler et al.*, 2008], displayed a region of significant positive SST-SSS correlations in the central to

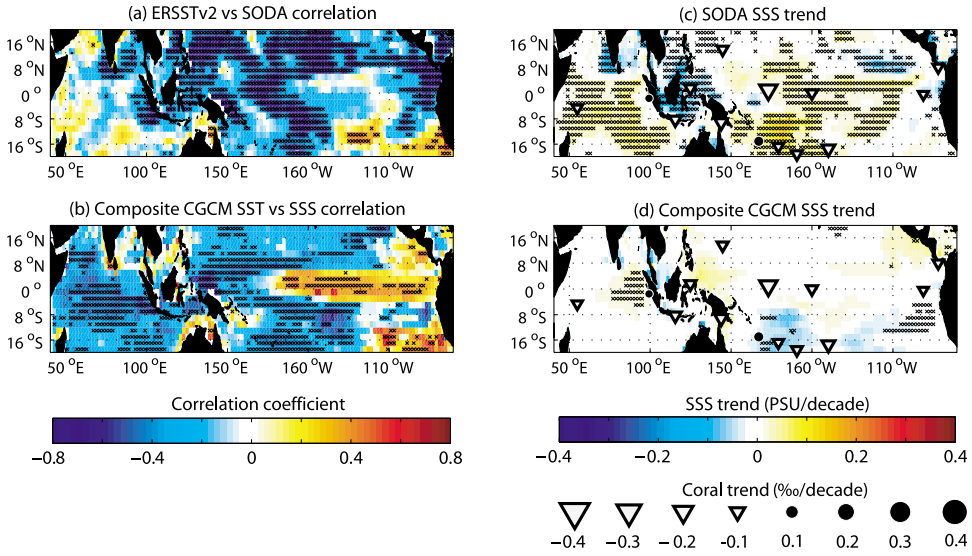

Figure 3. (left) Correlation of SST and SSS from 1958 to 1990 over the tropical Indo-Pacific in (a) instrumental SST and SSS: ERSSTv2 and SODA and (b) the 7 CGCMs analyzed here (weighted average). (right) SSS trend (PSU/decade) from 1958 to 1990 in (c) SODA SSS and (d) the 7 CGCMs (weighted average). The $\delta^{18}O_{coral}$ trends (‰/decade) over this period were also plotted for comparison. Hatching indicates significant correlation (Figure 3a), trend values (Figure 3c), or grid-boxes for which the mean value in the 7 models was significantly different from zero (Figure 3b and 3d) at the 95% confidence level. The models were interpolated to a common 2 × 2 degree latitude/longitude grid resolution and weighted based on their ability to capture tropical climate variability (1-Model Variability Index (MVI) [*Gleckler et al.*, 2008]) prior to averaging and significance testing (see Figure S2 for individual model patterns).

eastern tropical Pacific (Figure 3b). A similar pattern was observed in the unweighted composite. Second, the magnitude and direction of SSS trends simulated by these CGCMs were very different from instrumental SSS trends and from each other (cancelling each other in many regions of the composite) (Figures 3c, 3d, and S2). Thus, biases in the SSS trend and variability at the 23 coral sites (Figure 3d) may contribute to the discrepancy between observed and CGCM simulated coral trends over the 20th century.

7. Conclusions and Future Work

[22] A linear temperature- and salinity-driven model for $\delta^{18}O_{coral}$ captured the spatial and temporal pattern of ENSO and the linear trend observed in corals between 1958 and 1990. The negative $\delta^{18}O$ trend observed in corals had substantial contributions from both general warming (~60%) and regional freshening (~40%). When we drove this proxy model with CGCM output, we found differences between observed and simulated coral trends over the 20th century. Our work highlights potential biases in CGCM-simulated SSS fields, suggesting that the response of the tropical hydrological cycle to 20th-century climate forcing needs to be further investigated to improve our understanding of the evolution of tropical Pacific climate. Discrepancies between coral and CGCM trends may also result from variance in the observed coral dataset that is unexplained by the linear bivariate model. Further investigation of potential nonlinearities in how $\delta^{18}O_{coral}$ tracks climate, and coupling the proxy model presented here with isotope-enabled climate models, will provide useful tools to explore these discrepancies.

[23] **Acknowledgments.** We thank Joellen L. Russell, Jonathan T. Overpeck, Alexander W. Tudhope, J. Warren Beck, David Noone, and Heidi Barnett for helpful comments and support on this project. This research was supported by NOAA's Climate Change Data and Detection Program (award NA10OAR4310115 to JEG, MNE, and DMT and award NA08OAR4310682 to JEC), by the University of Arizona Department of Geosciences, and by the Institute of the Environment at the University of Arizona.

[24] The Editor thanks the two anonymous reviewers for their assistance in evaluating this paper.

References

Anchukaitis, K. J., M. N. Evans, A. Kaplan, E. A. Vaganov, M. K. Hughes, H. D. Grissino-Mayer, and M. A. Cane (2006), Forward modeling of regional scale tree-ring patterns in the southeastern United States and the recent influence of summer drought, *Geophys. Res. Lett.*, *33*, L04705, doi:10.1029/2005GL025050.

Ault, T. R., J. E. Cole, M. N. Evans, H. Barnett, N. J. Abram, A. W. Tudhope, and B. K. Linsley (2009), Intensified decadal variability in tropical climate during the late 19th century, *Geophys. Res. Lett.*, *36*, L08602, doi:10.1029/2008GL036924.

Brown, J., I. Simmonds, and D. Noone (2006), Modeling $\delta^{18}O$ in tropical precipitation and the surface ocean for present-day climate, *J. Geophys. Res.*, *111*, D05105, doi:10.1029/2004JD005611.

Brown, J., A. W. Tudhope, M. Collins, and H. V. McGregor (2008), Mid-Holocene ENSO: Issues in quantitative model-proxy data comparisons, *Paleoceanography*, *23*, PA3202, doi:10.1029/2007PA001512.

Carton, J. A., and B. S. Giese (2008), A reanalysis of ocean climate using Simple Ocean Data Assimilation (SODA), *Mon. Weather Rev.*, *136*, 2999–3017, doi:10.1175/2007MWR1978.1.

Carton, J. A., et al. (2000), A Simple Ocean Data Assimilation analysis of the global upper ocean 1950–1995. Part 1: Methodology, *J. Phys. Oceanogr.*, *30*, 294–309, doi:10.1175/1520-0485(2000)030<0294:ASODAA>2.0.CO;2.

Cole, J. E., and R. G. Fairbanks (1990), The Southern Oscillation recorded in the $\delta^{18}O$ of corals from Tarawa Atoll, *Paleoceanography*, *5*, 669–683, doi:10.1029/PA005i005p00669.

Cravatte, S., et al. (2009), Observed freshening and warming of the western Pacific Warm Pool, *Clim. Dyn.*, *33*(4), 565–589, doi:10.1007/s00382-009-0526-7.

Epstein, S., et al. (1953), Revised carbonate-water isotopic temperature scale, *Geol. Soc. Am. Bull.*, *64*(11), 1315–1326, doi:10.1130/0016-7606(1953)64[1315:RCITS]2.0.CO;2.

Evans, M. N., A. Kaplan, and M. A. Cane (2000), Intercomparison of coral oxygen isotope data and historical sea surface temperature (SST): Potential for coral-based SST field reconstructions, *Paleoceanography*, *15*(5), 551–563, doi:10.1029/2000PA000498.

Fairbanks, R. G., et al. (1997), Evaluating climate indices and their geochemical proxies measured in corals, *Coral Reefs*, *16*(5), S93–S100, doi:10.1007/s003380050245.

Gleckler, P. J., K. E. Taylor, and C. Doutriaux (2008), Performance metrics for climate models, *J. Geophys. Res.*, *113*, D06104, doi:10.1029/2007JD008972.

Guilyardi, E., et al. (2009), Understanding El Niño in ocean-atmosphere general circulation models: Progress and challenges, *Bull. Am. Meteorol. Soc.*, *90*(3), 325–340, doi:10.1175/2008BAMS2387.1.

Juillet-Leclerc, A., and G. Schmidt (2001), A calibration of the oxygen isotope paleothermometer of coral aragonite from Porites, *Geophys. Res. Lett.*, *28*, 4135–4138, doi:10.1029/2000GL012538.

Kaplan, A., et al. (1998), Analyses of global sea surface temperature 1856–1991, *J. Geophys. Res.*, *103*, 18,567–18,589, doi:10.1029/97JC01736.

LeGrande, A. N., and G. A. Schmidt (2006), Global gridded data set of the oxygen isotopic composition in seawater, *Geophys. Res. Lett.*, *33*, L12604, doi:10.1029/2006GL026011.

Lough, J. M. (2004), A strategy to improve the contribution of coral data to high-resolution paleoclimatology, *Palaeogeogr. Palaeoclimatol. Palaeoecol.*, *204*(1–2), 115–143, doi:10.1016/S0031-0182(03)00727-2.

McConnaughey, T. (1989), ^{13}C and ^{18}O isotopic disequilibrium in biological carbonates: I. Patterns, *Geochim. Cosmochim. Acta*, *53*, 151–162, doi:10.1016/0016-7037(89)90282-2.

Meehl, G. A., et al. (2007), Global climate projections, in *Climate Change 2007: the physical science basis. Contribution of Working Group I to the Fourth Assessment Report of the Intergovernmental Panel on Climate Change*, edited by S. Solomon et al., pp. 747–845, Cambridge Univ. Press, Cambridge, U. K.

Nurhati, I. S., K. M. Cobb, C. D. Charles, and R. B. Dunbar (2009), Late 20th century warming and freshening in the central tropical Pacific, *Geophys. Res. Lett.*, *36*, L21606, doi:10.1029/2009GL040270.

Overland, J. E., and R. W. Preisendorfer (1982), A significance test for principal components applied to a cyclone climatology, *Mon. Weather Rev.*, *110*, 1–4, doi:10.1175/1520-0493(1982)110<0001:ASTFPC>2.0.CO;2.

Rayner, N. A., D. E. Parker, E. B. Horton, C. K. Folland, L. V. Alexander, D. P. Rowell, E. C. Kent, and A. Kaplan (2003), Global analyses of sea surface temperature, sea ice, and night marine air temperature since the late nineteenth century, *J. Geophys. Res.*, *108*(D14), 4407, doi:10.1029/2002JD002670.

Roden, J. S., G. Lin, and J. R. Ehleringer (2000), A mechanistic model for interpretation of hydrogen and oxygen isotope ratios in tree-ring cellulose, *Geochim. Cosmochim. Acta*, *64*(1), 21–35, doi:10.1016/S0016-7037(99)00195-7.

Smith, T. M., and R. W. Reynolds (2004), Improved extended reconstruction of SST (1854–1997), *J. Clim.*, *17*, 2466–2477, doi:10.1175/1520-0442(2004)017<2466:IEROS>2.0.CO;2.

Smith, T. M., et al. (2008), Improvements to NOAA's historical merged land-ocean surface temperature analysis (1880–2006), *J. Clim.*, *21*, 2283–2296, doi:10.1175/2007JCLI2100.1.

Tolwinski-Ward, S., et al. (2011), An efficient forward model of the climate controls on interannual variation in tree-ring width, *Clim. Dyn.*, *36*, 2419–2439, doi:10.1007/s00382-010-0945-5.

Vaganov, E. A., M. K. Hughes, and A. V. Shashkin (2006), *Growth Dynamics of Tree Rings: Images of Past and Future Environments*, Springer, New York.

Vecchi, G. A., A. Clement, and B. J. Soden (2008), Examining the tropical Pacific's response to global warming, *Eos Trans. AGU*, *89*(9), doi:10.1029/2008EO090002.

Weber, J. N., and P. M. J. Woodhead (1972), Temperature dependence of oxygen-18 concentration in reef coral carbonates, *J. Geophys. Res.*, *77*, 463–473, doi:10.1029/JC077i003p00463.

T. R. Ault, J. E. Cole, and D. M. Thompson, Department of Geosciences, University of Arizona, Gould-Simpson Building #77, 1040 E. 4th St., Tucson, AZ 85721, USA. (thompsod@email.arizona.edu)

J. Emile-Geay, Department of Earth Sciences, University of Southern California, 3651 Trousdale Pkwy., Los Angeles, CA 90089, USA.

M. N. Evans, Department of Geology, University of Maryland, Geology Building, Room 1120, College Park, MD 20742, USA.